21st Australasian Fluid Mechanics Conference
Adelaide, Australia
10-13 December 2018

CFD simulations of vertical surface piercing circular cylinders and comparison against experiments

S. J. Keough[1,3], D. W. Stephens[2], A. Ooi[3], J. Philip[3] and J. P. Monty[3]

[1]Maritime Division
Defence Science and Technology Group, Fishermans Bend, Victoria 3207, Australia

[2]Applied CCM Pty Ltd, Ferntree Gully, Victoria 3156, Australia

[3]Department of Mechanical Engineering
University of Melbourne, Parkville, Victoria 3010, Australia

Abstract

When predicting the susceptibility of a submarine to above water detection, it is important to consider the impact of the wake generated by the periscope(s). Computational Fluid Dynamics (CFD) tools can be used to predict the physical size and shape of the wake, which can be combined with periscope models for input into detectability prediction models. For this application, it is important that CFD predictions of the wake are accurate not only in the mean calculations, but that the physical characteristics of the wake are captured at instantaneous snapshots in time.

In a previous experimental study, Keough et al. [10] presented time resolved measurements of the wake from vertical surface piercing cylinders, utilising an automated method of extracting these measurements as a function of time from video recordings of the experiment. In the present work, CFD simulations have been performed to model this experimental data set. The open source CFD software Caelus was used, with the improved Defence Science and Technology Group version of *vofSolver*—the multiphase volume of fluid solver. A numerical wave gauge is implemented in order to measure the free surface elevation during the simulation and this data is compared to bow wave data obtained from animations of the CFD results, using the same automated visual tracking technique utilised for the experimental measurements. Analysis of these time-resolved measurements is performed, comparing transient statistics and spectral characteristics of the CFD predictions against the experimental data.

Introduction

Computational Fluid Dynamics (CFD) is a useful tool for predicting flow in cases where experimental measurements can be difficult or costly to conduct, such as measuring the wake from a submarine periscope. A circular cylinder can be used as a simple proxy for a periscope moving through the free surface and several studies into the free surface flow around cylinders have been conducted both experimentally [7, 4, 5] and computationally [3, 11, 5]. CFD studies often focus on low Froude number flows, presumably to reduce the computational resource requirements of the simulation. Where higher Froude numbers have been investigated, the measurements are generally presented as mean or snapshot values and so transient fluctuations in the flow are not captured. For the purpose of predicting detectability of a periscope and its wake, it is important that the flow be accurate at snapshots in time and that transient variability be captured in order to predict the resulting variation in detectability over any given period of time.

In a previous study, Keough et al. [10] performed towing tank experiments up to a Froude number ($Fr_d = \frac{U}{\sqrt{gd}}$ where U is the velocity of the towed cylinder, d is the cylinder diameter and g is gravitational acceleration) of $Fr_d = 3.03$ and measured the bow wave height (D_1, defined by Hay [7] as the height of the water directly in front of the cylinder) as a function of time, capturing the transient fluctuations and allowing a detailed analysis of the flow, including a brief investigation into spectral characteristics. In the current study, CFD simulations are performed matching these experiments, with the D_1 measurement extracted using both a visual tracking method (as used in the experiments) and a numerical wave gauge. Collection of this time-resolved measurement allows analysis of the transient statistics as well as the spectral characteristics of the flow, for direct comparison against the experimental data. While it is difficult to compare snapshot information between different experiments (whether physical or simulated) comparison of the statistical and spectral characteristics of the transient flow provides a step toward validating the CFD model for such fluctuating flows.

Methodology

CFD Software and Numerical Method

For this study, the open source CFD software Caelus [1] has been used to simulate free surface flow around cylinders, utilising a modified version of *vofSolver*—the multiphase volume of fluid (VoF) solver—developed by the Defence Science and Technology Group. The incompressible Navier-Stokes equations are solved using the finite volume method, with turbulence modelled using the large eddy simulation (LES) method and a Smagorinsky sub-grid scale (SGS) model as described by Sidebottem et al. [14]. Free surface capturing is performed using a VoF method as detailed by Deshpande et al. [6]. It has been shown that the VoF method is an effective method of free surface capture, especially for flows with complex features such as breaking waves [12].

Case Setup

The simulations are set up to match, as best possible, the towing tank experiments at the Australian Maritime College [10], with a simulation domain of width 3.5 m, length 8 m and height 1.4 m. A relativistic frame is used to represent the cylinder being pulled through the towing tank, where the cylinder is held stationary and the fluids enter the inlet boundary at a speed equivalent to that of the moving cylinder. The side boundaries are set as fixed velocity to mimic a no-slip wall condition in the relativistic frame. A relaxation zone is used at the outlet boundary to prevent wave reflections from the wake and the simulation is initialised by accelerating the relative frame from stationary up to the required velocity, as described by Brady [3].

Meshing

The domain mesh is generated using the open source meshing

utility snappyHexMesh [8]. A coarse background mesh is refined at the flat water free surface location, a circular region around the cylinder and in the regions around and behind the cylinder where the wake will form. A brief mesh study was carried out by generating meshes of four different resolutions as detailed in Table 1. For all other simulations presented here, the "Fine" mesh was utilised.

Table 1: Details of each mesh used for the mesh study. Values provided are cell edge lengths for the background mesh (h_{bg}), free surface region (h_{fs}) and cylinder surface (h_{cyl}) as well as the total number of cells in the domain.

Mesh	Cell Edge Length (mm)			Total Cells
	h_{bg}	h_{fs}	h_{cyl}	
Fine	50	6.25	1.56	113,217,293
Medium	62.5	7.8	1.95	60,840,436
Coarse	80	10	2.5	30,977,260
Very Coarse	100	12.5	3.125	14,643,398

Free Surface Tracking

In the previous work [10], an automated video processing technique was utilised to extract D_1 measurements from towing tank experiments of cylinders being pulled through water. For consistency in analysis, the same technique is used here to measure the D_1 values predicted by the CFD simulations. A run-time function object is used to sample the free surface location at a rate of 100 Hz by interpolating the location of volume fraction $\alpha = 0.5$. At each sampling time, a wireframe mesh of the free surface is output with a number of triangles dependent on the density of the underlying domain mesh used for the CFD. Since a large number of cells are utilised to resolve the free surface in the CFD, this results in very large free surface wireframes that can be prohibitively slow to post-process on standard computer hardware. To speed up generating animations using these files, the wireframes are decimated using the vtkDecimatePro algorithm provided with the Visualisation Toolkit library [13]. The vtkDecimatePro algorithm is able to reduce the size of the wireframes by approximately 70% with negligible loss of topological information in the data, significantly improving processing times. Animations of the free surface flow are then generated using the open source visualisation software Paraview [2], before being processed using the visual tracking algorithm in order to extract the D_1 measurement data. Figure 1 shows an example frame of an animation. In the absence of scale markings on the cylinder, a digital ruler is used to calibrate the measurements.

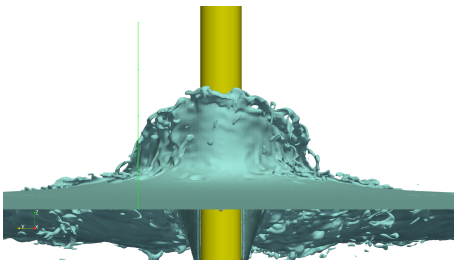

Figure 1: Screenshot of CFD results as visualised using Paraview. Animations are generated to allow measurement of bow wave height using the visual tracking algorithm.

The second method utilised for obtaining the bow wave height involved implementing a numerical wave gauge provided by the waves library [9]. The gauge is placed 1 mm directly in front of the cylinder and measures the surface elevation by integrating the volume fraction from the bottom to the top of the domain at the specified x-y location. By definition, the volume fraction is $\alpha = 1$ in the water phase and $\alpha = 0$ in the air phase, hence this integral sums to the z-axis location of the interface between the phases. This method relies on the assumption that a single interface exists along the line integral, which can reasonably be expected for the case of the bow wave directly at the front of the cylinder.

Results

Mesh Resolution Study

Figure 2 shows the measured non-dimensional bow wave height (D_1/d) over the length of the simulation (including initialisation) for each of the four mesh resolutions. Qualitative inspection immediately highlights that there is nearly no similarity in the fluctuating pattern between any of the results. This is to be expected when using LES turbulence modelling as refining the mesh will resolve smaller turbulent length scales, thus changing the predicted flow dynamics.

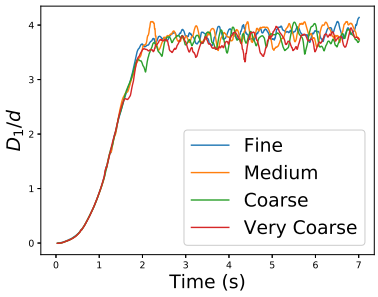

Figure 2: Non-dimensional bow wave height (D_1/d) measurements over 7 s of simulation time (including 2 s initialisation) at $Fr_d = 3.03$, for each mesh resolution.

Table 2 compares the mean, standard deviation and amplitude (difference between max. and min. observed values in the time sample, excluding initialisation) of each simulation. It can be seen that the coarser meshes predict a lower mean height, likely as a result of additional numerical dissipation due to the mesh. Both the "medium" and "fine" meshes predict similar mean height and amplitude, suggesting that at these resolutions, even though the transient results differ, the predictions are becoming statistically mesh independent.

Table 2: Mean, standard deviation and amplitude of the non-dimensional bow wave height (D_1/d) for each mesh resolution

Mesh	Mean	Std Dev	Amp
Fine	3.829	0.097	0.539
Medium	3.828	0.130	0.534
Coarse	3.725	0.146	0.915
Very Coarse	3.684	0.124	0.653

Time-Resolved Bow Wave Height

Repeating the analysis of the previous work [10] on the CFD simulations allows direct comparison with the data from the towing tank experiments, while also giving insight into the suitability of the two techniques used to track the bow wave height in the CFD.

Figure 3 shows the time resolved D_1/d measurement at each speed for the towing tank experiment along with the same measurement taken from the CFD simulation using both the video

tracking algorithm and the numerical wave gauge. Due to the significant time required for the CFD simulations to complete, each simulated experiment was run for a period of only 7 s, including the 2 s acceleration period. Since spectral analysis of the experimental results showed a broad peak between 1-10 Hz [10], it is expected that 5 s of simulation will be sufficient to display all of the relevant time scales in the flow. At each Froude number measured, a 5 s sample of the experimental data has been extracted, to allow direct comparison with the CFD over the same time frame.

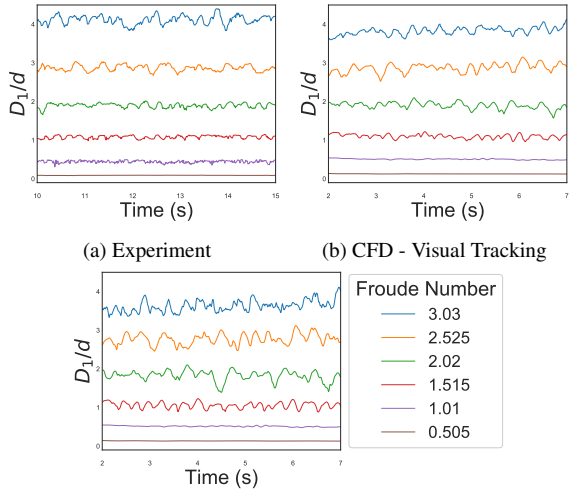

(a) Experiment (b) CFD - Visual Tracking

(c) CFD - Wave Gauge

Figure 3: Time resolved D_1/d measurements over a 5 s period from (a) towing tank experiments [10], (b) CFD simulations using visual bow-wave tracking and (c) CFD simulations using a numerical wave gauge.

Table 3 shows the same statistical characteristics presented in the mesh study for each of the curves represented in Figure 3. In general, the similarity between the mean values at each Froude number suggests that the CFD is able to accurately predict the height of the bow wave.

Table 3: Non-dimensional bow-wave height (D_1/d) statistics for experimental (Exp) and CFD results using visual tracking (CFD-VT) and using a numerical wave gauge (CFD-WG).

Fr_d	Dataset	Mean	Std Dev	Amp
0.505	Exp	0.084	0.005	0.38
	CFD-VT	0.127	0.002	0.13
	CFD-WG	0.133	0.002	0.14
1.01	Exp	0.458	0.030	2.63
	CFD-VT	0.506	0.014	0.61
	CFD-WG	0.512	0.014	0.68
1.515	Exp	1.089	0.039	0.228
	CFD-VT	1.099	0.054	0.257
	CFD-WG	1.058	0.078	0.348
2.02	Exp	1.899	0.062	0.414
	CFD-VT	1.899	0.085	0.522
	CFD-WG	1.824	0.133	0.708
2.525	Exp	2.885	0.076	0.430
	CFD-VT	2.872	0.113	0.628
	CFD-WG	2.772	0.141	0.663
3.03	Exp	4.131	0.121	0.632
	CFD-VT	3.828	0.096	0.526
	CFD-WG	3.625	0.146	0.781

At the lower Froude numbers (0.505 and 1.01) when there is little variation in the bow wave height over time, the CFD predicts a slightly higher and more steady bow wave. It is likely in this case that error is present in the experimental results. The experimental error is expected to be approx. ± 5 mm, mostly due to difficulty in locating the peak of the bow wave against the black background of the scale markings on the cylinder. This source of error does not occur in the generated images of the CFD result, as seen in Figure 4.

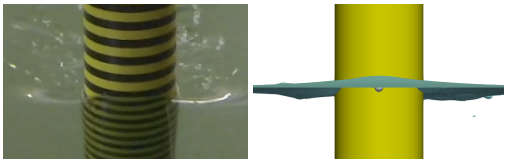

Figure 4: Screenshots of video used for visual tracking of the bow wave for towing tank experiments (left) and CFD simulations (right) at $Fr_d = 0.505$. Scale markings that can introduce experimental error in height tracking are not present in the CFD results.

There is a noticeable difference between the results of the visual tracking and wave gauge measurement methods. As the Froude number increases, the wave gauge measures a slightly lower mean height and a larger amplitude in the variation. This is due to the video tracking algorithm taking a root mean square of the bow wave height in each pixel column across a width of approximately 40 mm at the front of the cylinder. It also captures the highest point in line of sight between the camera and cylinder, irrespective of the distance the free surface is away from the cylinder at that point. The result of this averaging process is that the fluctuations measured will be slightly smaller and the calculated mean is likely to be slightly higher, as higher points in the bow wave immediately surrounding the centre of the cylinder are included in the measurement (see Figure 5).

Figure 5: Screenshot of a CFD result highlighting how the averaging processing in the visual tracking algorithm can occasionally measure a D_1 value (red dot) higher than the bow wave height directly at the front of the cylinder, when the free surface in the immediate vicinity is higher.

By comparison, the numerical wave gauge measures the free surface height only at a single point in the x-y coordinate plane, in this case 1 mm directly in front of the cylinder. This measurement technique is likely to give a more accurate measurement of the "bow wave height" as predicted by Bernoulli's equation, based on the stagnation pressure at the front of the cylinder [4, 10]. For the purpose of comparing the CFD results with the experimental data as available, the video tracking method provides a better direct comparison, but it is apparent that higher quality experimental data could be obtained by implementing a wave gauge at the front of the cylinder.

At the highest Froude number presented here, the CFD underpredicts the mean height more significantly than in the other measurements. As the Froude number increases, the dissipation due to turbulence and numerical effects is likely to increase, increasing the likelihood of the CFD over-predicting the energy dissipation and thus under-predicting the height.

Power Spectral Density

Power Spectral Density (PSD) was estimated for each set of data using the same technique implemented in the previous work [10], with the exception that instead of averaging across 5 s windows, only a single sample of 5 s was analysed, as this represented the full length of the CFD data available (excluding the initialisation period). To maintain a consistent analysis, only the 5 s subset of the experimental data shown in Figure 3a is used to estimate the PSD in the results shown here.

Figure 6 shows the PSD for Froude numbers greater than 1.5 and it can be seen that each of the curves shows the same broad peak between 1-10 Hz with a dominant frequency between 2-4 Hz. While each curve exhibits a noticeable amount of noise due to the small amount of data and lack of windowed averaging in the processing, the clear similarity between the experimental result and the CFD result from the visual tracking method shows that the CFD is accurately predicting the transient fluctuations in the bow wave height. The CFD result from the wave gauge measurement exhibits a spectral curve with the same general shape and dominant frequencies, but shows slightly higher values across most frequencies. This is to be expected as the amplitude of fluctuations measured by the wave gauge is higher, for reasons explained earlier.

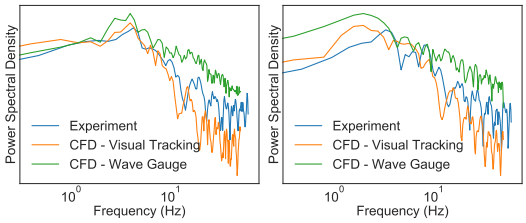

(a) $Fr_d = 1.52$ (b) $Fr_d = 2.02$

(c) $Fr_d = 2.52$ (d) $Fr_d = 3.03$

Figure 6: Non-dimenstional power spectral density estimates at Froude numbers of (a) 1.52, (b) 2.02, (c) 2.52 and (d) 3.03. Each plot compares the PSD of the towing tank experiment and the CFD simulation, including both visual tracking and wave gauge measurement of the CFD results.

Conclusions

CFD simulations implementing an LES turbulence model with a Smagorinsky SGS model and VoF free surface capturing were completed matching towing tank experiments of cylinders moving though a free surface from previous work [10]. Two methods of tracking the bow wave height during the simulation were implemented, a visual tracking method identical to that used to extract measurements from video of the experiment, and a numerical wave gauge. It was seen that at higher Froude numbers, the visual tracking technique is likely to slightly over predict the mean height, while under predicting the amplitude of transient fluctuations, when compared with the data from the wave gauge. A mesh resolution study suggested that while consistency in the time-resolved measurements could not be achieved on different meshes, the transient statistics began to approach mesh independence with mesh cell edge lengths at the cylinder of <2 mm. Comparing the transient statistics and power spectral density estimates of the bow wave height for both the towing tank experiment and the CFD suggests that the CFD is accurately predicting both the mean height and the frequency and amplitude of fluctuations. At higher Froude numbers, the CFD appears to over predict the dissipation, resulting in slightly under predicting the height of the bow wave.

References

[1] Applied CCM, *Caelus: Computational Mechanics Library (Version 7.04) [Software]*, Applied CCM, 2017, available at URL `http://www.caelus-cml.com`.

[2] Ayachit, U., The paraview guide: A parallel visualization application. kitware, 2015, isbn 978-1930934306.

[3] Brady, P., *An investigation of free surface hydraulic structures using large eddy simulation and computational fluid dynamics*, Ph.D. thesis, University of Technology Sydney, 2011.

[4] Chaplin, J. and Teigen, P., Steady flow past a vertical surface-piercing circular cylinder, *Journal of Fluids and Structures*, **18**, 2003, 271–285.

[5] Conway, A. S. T., Binns, J. R., Ranmuthugala, D. and Renilson, M., Experimental and numerical analysis of submarine mast surface wakes, in *Pacific International Maritime Conference*, 2015, 1–12.

[6] Deshpande, S., Anumolu, L. and Trujillo, M. F., Evaluating the performance of the two-phase flow solver interFoam, *Computational Science and Discovery*, **5**, 2012.

[7] Hay, A. D., *Flow about semi-submerged cylinders of finite length*, Princeton University, 1947.

[8] Jackson, A., A comprehensive tour of snappyhexmesh, in *7th OpenFOAM Workshop Lecture, Darmstadt*, 2012.

[9] Jacobsen, N. G., Fuhrman, D. R. and Fredsøe, J., A wave generation toolbox for the open-source cfd library:openfoam®, *International Journal for Numerical Methods in Fluids*, **70**, 2012, 1073–1088.

[10] Keough, S. J., Kermonde, I. L., Amiet, A., Philip, J., Ooi, A., Monty, J. P. and Anderson, B., Time Resolved Measurements of Wake Characteristics from Vertical Surface-Piercing Circular Cylinders, in *Proceedings of the 20th Australasian Fluid Mechanics Conference*, Australasian Fluid Mechanics Society, 2016, 8–11.

[11] Koo, B., Suh, J., Yang, J. and Stern, F., Simulation of two-phase flow past a vertical surface-piercing circular cylinder, in *ASME 2010 3rd Joint US-European Fluids Engineering Summer Meeting collocated with 8th International Conference on Nanochannels, Microchannels, and Minichannels*, American Society of Mechanical Engineers, 2010, 435–445.

[12] Rhee, S., Makarov, B. P., Krishinan, H. and Ivanov, V., Assessment of the volume of fluid method for free-surface wave flow, *Journal of Marine Science and Technology*, **10**, 2005, 173 – 180.

[13] Schöberl, J., Martin, K. and Lorensen, B., *The Visualization Toolkit (4th ed.)*, Kitware, 2006, ISBN: 978-1-930934-19-1.

[14] Sidebottom, W., Ooi, A. and Jones, D., A parametric study of turbulent flow past a circular cylinder using large eddy simulation, *J Fluids Eng*, **137**.